Femtosecond laser activation of surface reactions

R.J. Finlay, S. Deliwala, J.R. Goldman, T.H. Her, W.D. Mieher, C. Wu, and E. Mazur

Department of Physics and Division of Applied Sciences,
Harvard University, Cambridge, MA 02138

Abstract

Laser induced formation of CO_2 and desorption of O_2 are initiated with femtosecond and picosecond laser excitation of a Pt(111) surface prepared with coadsorbed CO and O_2 at 90 K. The nonlinear fluence dependent reaction yields were measured for 267, 400, and 800 nm wavelengths, and for pulse durations from 80 fs to 3.6 ps. Two-pulse correlation experiments measuring total O_2 desorption yield versus time delay between 80 fs pulses show a 0.9 ps HWHM central peak and a slower 0.1 ns timescale. At 267 nm the relative yields of O_2 and CO_2 are found to depend on fluence. Comparison of results at different wavelengths and pulsewidths shows that nonthermalized surface electrons play a role in the laser-induced surface chemistry.

Keywords: ultrafast, femtosecond, laser, surface, reaction, oxygen, carbon dioxide, platinum, Ti:sapphire, time resolved

1. Introduction

In the past 5 years, subpicosecond laser pulses have been used to investigate desorption of adsorbed molecules from metal surfaces.[1-5] These experiments demonstrated highly nonlinear dependences of the desorption yield on the laser fluence. Two-pulse correlation measurements show subpicosecond time-scales for the laser-induced excitation responsible for desorption[2, 4, 5] and for the desorption process itself.[6] The surface electron temperature easily reaches several thousand Kelvin over the duration of a subpicosecond laser excitation pulse and then cools on a time-scale of 1-3 ps[2, 5-7] Both the nonlinear fluence dependence and the short time scale of the desorption have been previously attributed to hot electrons in the metal.[1-10]

We have studied the desorption of O_2 and formation of CO_2 initiated with subpicosecond laser pulse excitation of O_2/Pt(111) and coadsorbed CO/O_2/Pt(111) surfaces at 90 K in ultrahigh vacuum. O_2

0-8194-1906-0/95/$6.00

desorption and laser-induced CO_2 formation (followed by desorption) are detected with a mass spectrometer. The surface chemistry of the O_2/Pt(111) and CO/O_2/Pt(111) systems has been well characterized.[11-15] The photochemistry of these systems has been studied with arc lamp irradiation,[13, 14] and with nanosecond[3, 16] and subpicosecond[3, 4] laser pulses. We report the fluence dependence of the desorption yield of O_2 and CO_2 at 267, 400, and 800 nm over a range of pulsewidths from 80 fs to 3.6 ps. The experiments presented in this paper extend the range of excitation conditions used in previously published studies. We also present two-pulse correlation data obtained with 80-fs pulses at 800 nm using delays up to 75 ps. The results present convincing evidence that nonthermalized highly-excited electrons play a significant role in the desorption and surface reaction processes.

2. Experiment

The Pt(111) surface is cleaned and prepared in an ultrahigh vacuum system using established methods.[14] The clean Pt surface is dosed to saturation (0.44 monolayers[17]) with $^{18}O_2$ utilizing a capillary array to minimize the O_2 background pressure during the experiment. For the mixed layer CO/O_2/Pt(111), a 3×10^{-6} Torr-s background exposure of $^{12}C^{18}O$ follows the $^{18}O_2$ dose. O_2 chemisorbs molecularly on Pt(111) below 100 K. Two species observed in vibrational spectroscopy have been assigned to O_2 bound in atop and bridge sites with the O–O bond axis parallel to the surface and bond orders of about 1.[17] In the presence of preadsorbed O_2, CO has been observed in the atop sites.[14]

The regeneratively amplified Ti:Sapphire laser system used in these experiments was designed in our laboratory and employs chirped-pulse amplification and all-reflective optics. Pulses of 70-fs duration, 0.5-mJ energy, and 800-nm wavelength are produced at a 1-kHz repetition rate. By adjusting the pulse compressor, longer chirped pulses are obtained. Frequency-doubled 400-nm pulses are produced in a 1-mm long LBO crystal yielding 0.1-mJ pulses of 0.2-ps duration. Sum-frequency mixing of the 800 and 400-nm pulses in a 0.3-mm long BBO crystal, yields 17-μJ pulses at 267 nm. Based on the group velocities of the 400 and 800-nm pulses in BBO, we estimate a pulsewidth of 0.35 ps for the 267-nm pulses.

The fluence is calibrated for each data run by measuring the energy and spatial profile of the laser pulses. The energy is measured with a photodiode referenced to a calibrated pyroelectric detector. Typical shot-to-shot energy fluctuations are 2% at 800 nm, 5% at 400 nm, and 10% at 267 nm. A CCD camera measures the profile of the 800 and 400-nm pulses. The profile of the 267-nm pulses is measured by scanning a 25μm pinhole through the beam. The camera or the pinhole are mounted outside the vacuum

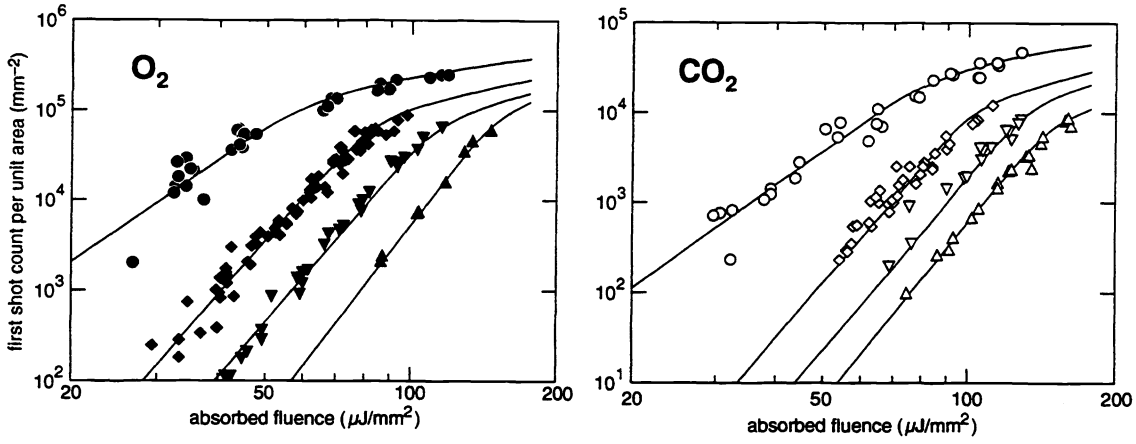

Figure 1: First shot yields for O_2 (solid symbols) and CO_2 (open symbols) as a function of absorbed fluence for 100 fs (diamonds), 0.6 ps (inverted triangles), and 3.6 ps (triangles) at 800 nm, and for 0.2 ps pulses at 400 nm (circles). The slopes are 6.5 ± 0.4 for 800 nm and 3.8 ± 0.5 for 400-nm data below saturation.

chamber at a point along the beam path equivalent to the sample location. The absorbed center fluence F is reported after fitting the measured spatial profile to an elliptical Gaussian function. For all wavelengths the absorbed fluence (*i.e.*, the incident fluence times the absorption of platinum[18] is in the range 10-200 $\mu J/mm^2$. For 400 and 800-nm pulses, the fluence is varied by changing the total incident energy with a half-wave plate and a polarizer. At 267 nm, the incident energy is held constant, and a lens is displaced to change the spot size on the sample. Every time the lens is moved, a new measurement of the spot size is made.

The desorption and reaction yields were measured as functions of laser fluence, wavelength, pulse duration, and pulse sequence. The data presented here consist of the integrated mass spectrometer signal detected for the first laser excitation pulse incident on a fresh spot on the sample. The complete data sets each include the desorption signal for 200 laser shots at a fixed sample location. Between runs of various laser conditions, the sample is translated by twice the FWHM of the irradiated area. When the entire sample has been used, the sample is cleaned and redosed. A negatively biased grid in front of the mass spectrometer shields the sample from stray electrons from the ionizer. A mechanical shutter is used to increase the time interval between successive laser shots to 0.4 s to allow the mass spectrometer signal to return to the background.

Figure 1 shows the desorption (left) and reaction (right) yields per unit area induced with 800-nm pulses of three durations and with short 400-nm pulses. Each data point represents the yield obtained

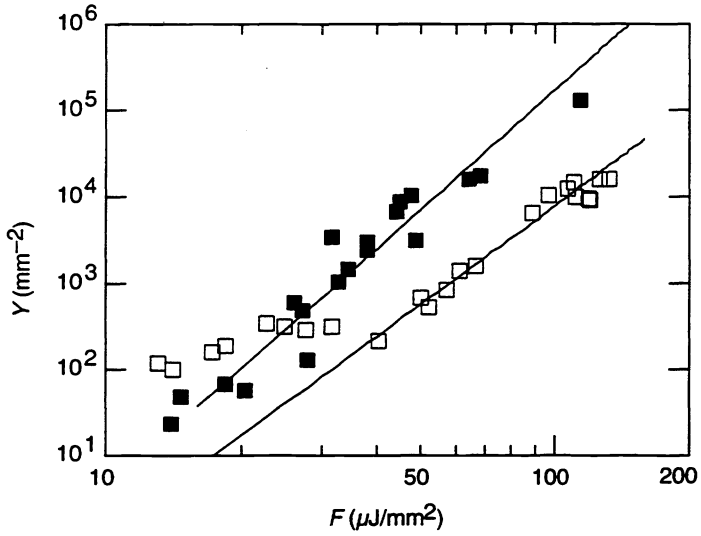

Figure 2: First shot yield of O_2 (solid squares) and CO_2 (open squares) at 267 nm. Note the change in slope for CO_2 at approximately 40 $\mu J\ mm^{-2}$.

from the first laser shot taken at a fresh spot on the Platinum sample. At 800 nm, the steep slope of the data, 6.5±0.4 for both O_2 and CO_2, is unchanged with pulsewidth. The nearly identical fluence dependence of the O_2 and CO_2 data provides strong evidence for a common excitation mechanism for desorption of O_2 and formation of CO_2. The ratio in desorption yield of O_2 to CO_2 is about 10, in sharp contrast with the ratio of 0.5 found with nanosecond irradiation.[3] The curves through the data are a power law relating yield to fluence, $Y \propto F^p$ at low fluences. At high fluences, the fit flattens out reflecting finite number of molecules available within the area illuminated by the laser.[19]

Figure 1 also shows the desorption and reaction yields with 400-nm, 0.2-ps pulses. The slope of the data is 3.8±0.5 for both O_2 and CO_2. The ratio of O_2 to CO_2 produced is near 10.

The desorption and reaction yields induced by 267-nm pulses are graphed in Figure 2. At high fluence, there is a nonlinear relationship between the yield and fluence: the lines through the O_2 and CO_2 data have slopes of 4.5 and 3.8 respectively. In this high fluence regime, the ratio of O_2 to CO_2 yield is close to 10. At low fluence, there is a change in the slope of the CO_2 product yield, allowing the CO_2 reaction product to exceed the O_2 product at low fluences. We have not been able to resolve any change in the slope of the O_2 data in the range of fluences studied to date. The reaction and desorption yields are equal near 25 $\mu J/mm^2$ absorbed fluence at 267 nm.

The pulsewidth dependence of the yield in Figure 1 motivates further study of the time dependence of the excitation. We measured the total desorption yield of two 80-fs, 800-nm pulses as a function

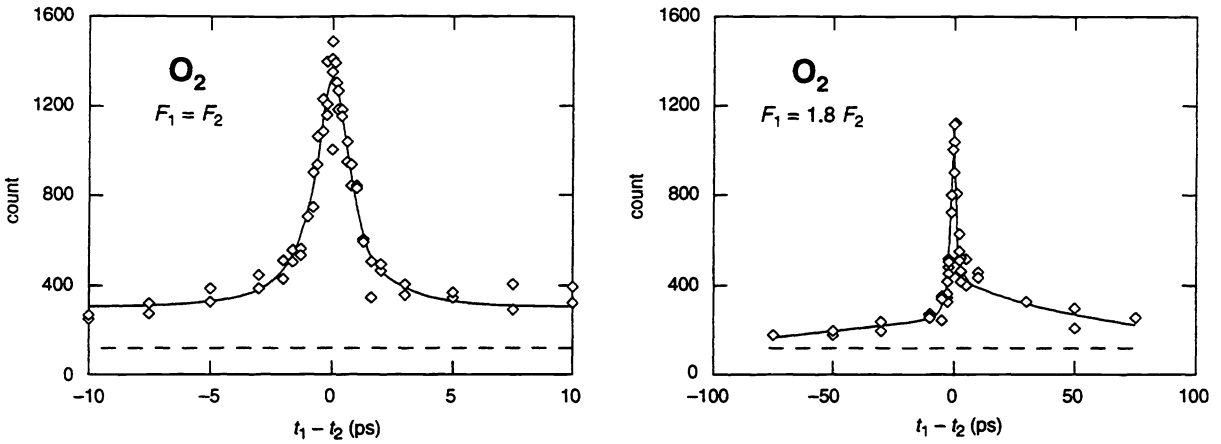

Figure 3: Desorption yield versus time delay $t_1 - t_2$ between two 80-fs excitation pulses at 800-nm for pulses of equal (left) and unequal (right) absorbed fluences. The dashed lines denote $Y(t_1 - t_2 = \pm\infty)$. In both cases the width of the central peak is 1.8 ps. For unequal fluences the desorption yield is enhanced when the weaker pulse arrives first($t_1 - t_2 > 0$). The desorption yield is still enhanced after 75 ps.

of the delay $t_1 - t_2$ between them. With equal absorbed fluence in the two pulses, the correlation is symmetric (Figure 3, left); with unequal fluences, an asymmetry appears in the wings which has been previously observed (Figure 3, right). The solid lines through the data are aids to determine the 1.8 ps full width at half maximum of the central peaks. The central peak was attributed to the cooling of the hot substrate electrons which are strongly coupled to the vibrations of the adsorbate.[2, 4, 5] The dashed line shows the total yield when the two pulses act independently, *i.e.*, when $t_1 - t_2 \rightarrow \pm\infty$. The observed 0.1-ns decay time of the wings, however, provides new information. It indicates that the excitation lasts longer than the electron-adsorbate,[7, 9] electron-lattice,[2, 5-7, 20] and lattice-adsorbate[21] relaxation times. The only remaining equilibration process is the cooling of the surface to the bulk, which occurs on roughly the same time-scale as the decay of the wings.

3. Discussion

The evolution of the electron and lattice temperatures following short pulse irradiation was described by Anisimov et. al.[20] with two coupled differential equations. Numerous authors have applied solutions of these equations to describe the evolution of the temperature of the substrate electrons in femtochemistry experiments.[1-5] In particular, Ho and coworkers fit the form of the central peak in the two-pulse correlation experiment using a model based on coupling of the hot, thermalized electrons to adsor-

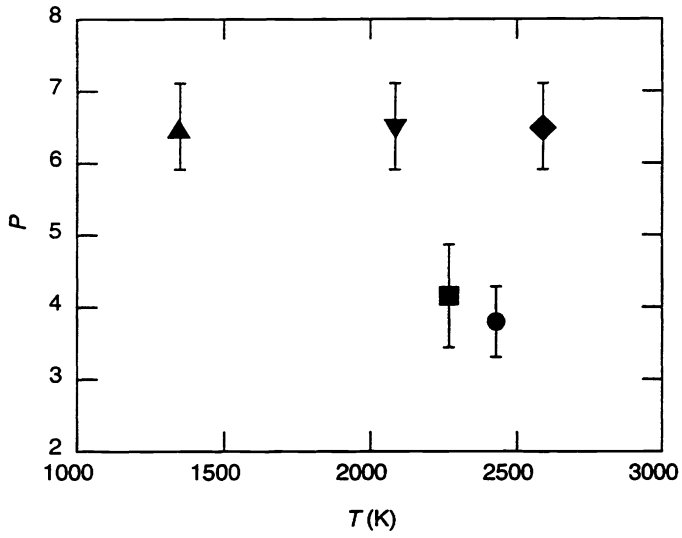

Figure 4: Power law exponent vs. calculated peak electron temperatures. (triangle 3.6 ps, inverted triangle 0.6 ps, and diamond 100 fs at 800 nm; circle 0.2 ps at 400 nm; and square 0.35 ps at 267 nm).

bate vibrational modes based on an experimentally determined coupling constant.[22,23]

The equations of Anisimov were solved at the surface using the physical constants of Pt, at 50 μJ/mm^2 absorbed fluence, for the pulse durations and wavelengths used in the experiment: 800-nm pulses of 100-fs, 0.6-ps, and 3.6-ps durations; 400-nm pulses of 0.2-ps duration; and 267-nm pulses of 0.35-ps duration. In the calculation, the various pulses lead to different peak electron temperatures primarily because of the different pulse durations involved. In Figure 4 power laws determined from the data of Figures 1 and 2 are plotted against the corresponding peak surface electron temperatures reached in the numeric simulations. Changes in absorption depth with photon energy are small for Pt over this range of photon energies, and thus do not have a substantial impact on the peak electron temperatures. The different reflectivity of the Pt at the various wavelengths is not relevant since the calculation is concerned with a fixed absorbed fluence. Changes in the physical constants of Pt assumed in the calculation would be expected to change the absolute results of the electron temperature calculation, but not the general behavior.

The distribution of data in Figure 4 show that there is no correlation between power law, p, and peak surface electron temperature. The data of Figures 1 and 2 show that simple power laws describe the yield over a wide range of fluences, pulse durations, and wavelengths. Thus the unsatisfactory relationship between power law and electron temperature indicates an unsatisfactory relationship between reaction yield and electron temperature. This observation challenges the assumption that a thermalized electron distribution solely governs the desorption. The wavelength dependence may arise because pho-

tons of different energies excite substrate electrons to different positions in the Pt band structure. Since electrons thermalize in less than a picosecond, a short time scale for the excitation process follows naturally.

Previous work with continuous wave (cw) illumination in the ultraviolet using an arc lamp source[14], and nanosecond laser illumination[3] reported CO_2 to O_2 yields in the ratio 0.5. The present result reaches this regime in which the reaction product dominates the simple desorption product using ultrashort (0.35 ps) laser pulses rather than cw or nanosecond illumination. It is probable that the change in the branching ratio and the decrease in the nonlinearity of the yield reflect a change in the reaction mechanism. This rudimentary control of branching ratio is expected to have practical importance in the study of time-resolved surface reaction dynamics, where conditions under which an ultra-short laser pulse can initiate a surface reaction (rather than simple desorption) are desirable.

4. Conclusion

Summarizing, the following observations emerge from these experiments:

(1) Comparison of data obtained at different wavelengths show a clear dependence of desorption yield on wavelength. This behavior cannot be adequately described by current theoretical models, which predict a dependence on absorbed fluence but not on wavelength. The observed wavelength dependence therefore calls for models that incorporate nonthermal electron distributions.

(2) The desorption yield decreases sharply with increasing pulse duration, but the power law exponent remains nearly the same. Changes in the pulse duration affect the competition between the excitation rate and the thermalization and cooling processes. An increase in pulse duration will result in a lower nonthermalized electron density and a lower electron temperature. Both of these effects could contribute to a decrease in the observed yield.

(3) In addition to the 1.8 ps central peak, the two-pulse experiments show a 0.1-ns decay time exceeding all relaxation times except the cooling of the surface to the bulk temperature. The observation of a two-pulse correlation signal on such a long time scale implies that the temperature of the surface plays a role in the femtosecond-laser-induced desorption process.

(4) Ultrashort UV laser pulses (267 nm) can be used to access two reaction regimes. At high fluence, a nonlinear dependence of yield on fluence is observed in which the O_2 product exceeds the CO_2 product by a factor of ≈ 10. At less than 25 $\mu J\ mm^{-2}$ of UV fluence, CO_2 production exceeds O_2 desorp-

tion.

5. Acknowledgments

This research is supported by the Army Research Office under Contract DAAL03-92-G-0238 and the Joint Services Electronics Program under Contract N00014-89-J-1023. R.J.F. is supported by the Natural Science and Engineering Research Council of Canada. J.R.G. acknowledges support from AASERT Fellowship DAAL03-92-G-0196. Generous support from Perkin-Elmer Physical Electronics, and ConOptics Inc. is gratefully acknowledged. Continuum Corporation provided financial support to R.J.F. to attend SPIE 1995.

6. References

1. J. A. Prybyla, T. F. Heinz, J. A. Misewich, M. M. T. Loy, and J. H. Glownia, Phys. Rev. Lett. vol. 64, 1537 (1990).
2. F. Budde, T. F. Heinz, M. M. T. Loy, J. A. Misewich, F. de Rougemont, and H. Zacharias, Phys. Rev. Lett. vol. 66, 3024 (1991).
3. F.-J. Kao, D. G. Busch, D. Gomes da Costa, and W. Ho, Phys. Rev. Lett. vol. 70, 4098 (1993).
4. F.-J. Kao, D. G. Busch, D. Cohen, D. Gomes da Costa, and W. Ho, Phys. Rev. Lett. vol. 71, 2094 (1993).
5. J. A. Misewich, A. Kalamarides, T. F. Heinz, U. Höfer, and M. M. T. Loy, J. Chem. Phys. vol. 100, 736 (1994).
6. J. A. Prybyla, H. W. K. Tom, and G. D. Aumiller, Phys. Rev. Lett. vol. 68, 503 (1992).
7. F. Budde, T. F. Heinz, A. Kalamarides, M. M. T. Loy, and J. A. Misewich, Surf. Sci. vol. 283, 143 (1993).
8. R. R. Cavanagh, D. S. King, J. C. Stephenson, and T. F. Heinz, J. Phys. Chem. vol. 97, 786 (1993).
9. J. A. Misewich, T. F. Heinz, and D. M. Newns, Phys. Rev. Lett. vol. 68, 3737 (1992).
10. D. M. Newns, T. F. Heinz, and J. A. Misewich, Prog. of Theo. Phys. vol. Suppl No. 106, 411 (1991).
11. T. Matsushima, Surf. Sci. vol. 123, L663 (1982).
12. T. Matsushima, Surf. Sci. vol. 127, 403 (1983).
13. W. D. Mieher, and W. Ho, J. Chem. Phys. vol. 91, 2755 (1989).
14. W. D. Mieher, and W. Ho, J. Chem. Phys. vol. 99, 9279 (1993).

15. K.-H. Allers, H. Pfnür, P. Feulner, and D. Menzel, J. Chem. Phys. vol. 100, 3985 (1994).
16. V. A. Ukraintsev, and I. Harrison, J. Chem. Phys. vol. 96, 6307 (1992).
17. H. Steininger, S. Lehwald, and H. Ibach, Surf. Sci. vol. 123, 1 (1982).
18. J. H. Weaver, C. Krafka, D. W. Lynch, and E. E. Koch, Optical Properties of Metals. Part. 1, Physics Data; (Fachinformationszentrum Energie, Physik, Mathematik, Karlsruhe, 1981).
19. S. Deliwala, R. J. Finlay, J. R. Goldman, T. H. Her, W. D. Mieher, and E. Mazur, Chem. Phys. Lett. (In Press) vol. (1995).
20. S. I. Anisimov, B. L. Kapeliovich, and T. L. Perel'man, Sov. Phys. JETP vol. 39, 375 (1974).
21. T. A. Germer, J. C. Stephenson, E. J. Heilweil, and R. R. Cavanagh, Phys. Rev. Lett. vol. 71, 3327 (1993).
22. S. Gao, D. G. Busch, and W. Ho, Surf. Sci. Lett. (In Press) (1995).
23. D. G. Busch, S. Gao, R. A. Pelak, M. F. Booth, and W. Ho, Phys. Rev. Lett. (In Press) (1995).